

**PLEASE COMPLETE THE PUBLICATION FEE CONSENT FORM BELOW
AND
RETURN TO THE PRODUCTION EDITOR WITH YOUR PROOF CORRECTIONS**

Please return this completed form and direct any questions to the Wiley Journal Production Editor at GRLprod@wiley.com.

To order OnlineOpen, you must complete the OnlineOpen order form at:

https://authorservices.wiley.com/bauthor/onlineopen_order.asp

Authors who select OnlineOpen will be charged the standard OnlineOpen fee for your journal, but excess publication fees will still apply, if applicable. **If your paper has generated excess publication fees, please complete and return the form below in addition to completing the OnlineOpen order form online (excess fees are billed separately).** If you would like to choose OnlineOpen and you have not already submitted your order online, please do so now.

YOUR ARTICLE DETAILS

Journal: *Geophysical Research Letters*

Article: Zhang, X., Leonardi, N., Donatelli, C., & Fagherazzi, S. (2020). Divergence of sediment fluxes triggered by sea-level rise will reshape coastal bays. *Geophysical Research Letters*, 47, e2020GL087862. <https://doi.org/10.1029/2020GL087862>

OnlineOpen: No **Words:** 4,221 **Tables:** 0 **Figures:** 4 **Total Publishing Units:** 12

Journal Base Fee: \$500
Excess Publishing Units: 0@ \$125 \$0
Publication Fee Total: USD \$500

Please provide the information requested below.

Bill to:

Name: _____
Institution: _____
Address: _____
Phone: _____ **Email:** _____
Signature: _____ **Date:** _____

An invoice will be mailed to the address you have provided once your edited article publishes online in its final format. Please include on this publication fee form any information that must be included on the invoice.

Publication Fees and Length Guidelines:

<http://publications.agu.org/author-resource-center/>

Frequently Asked Billing Questions:

[http://onlinelibrary.wiley.com/journal/10.1002/\(ISSN\)2169-8996/homepage/billing_faqs.pdf](http://onlinelibrary.wiley.com/journal/10.1002/(ISSN)2169-8996/homepage/billing_faqs.pdf)

Purchase Order Instructions:

Wiley must be listed as the contractor on purchase orders to prevent delay in processing invoices and payments.

Author Query Form

Journal: Geophysical Research Letters

Article: grl_60728

Dear Author,

During the copyediting of your paper, the following queries arose. Please respond to these by annotating your proofs with the necessary changes/additions.

- If you intend to annotate your proof electronically, please refer to the E-annotation guidelines.
- If you intend to annotate your proof by means of hard-copy mark-up, please use the standard proofing marks. If manually writing corrections on your proof and returning it by fax, do not write too close to the edge of the paper. Please remember that illegible mark-ups may delay publication.

Whether you opt for hard-copy or electronic annotation of your proofs, we recommend that you provide additional clarification of answers to queries by entering your answers on the query sheet, in addition to the text mark-up.

Query No.	Query	Remark
Q1	AUTHOR: Please fill out the Publication Fee Consent Form in these proofs (including complete mailing address) and return to the Production Editor with your proofs.	
Q2	AUTHOR: Please verify that the linked ORCID identifiers are correct for each author.	
Q3	AUTHOR: Please confirm that forenames/given names (blue) and surnames/family names (vermilion) have been identified correctly.	
Q4	AUTHOR: Please note that your references and their citations have been edited according to APA/AGU style, available at https://publications.agu.org/agu-grammar-and-style-guide/ .	
Q5	AUTHOR: Please provide publisher location for Reference “Horstman et al., 2013”.	
Q6	AUTHOR: Please provide the name of the publisher for Reference “Horstman et al., 2013”.	
Q7	AUTHOR: Please provide the chapter/article page numbers.	
Q8	AUTHOR: Please provide first page and last page for reference Lance et al. (2019).	
Q9	AUTHOR: Please provide publisher location for Reference “Stevenson et al., 1986”.	

Please confirm that the funding sponsor list below was correctly extracted from your article: that it includes all funders and that the text has been matched to the correct FundRef Registry organization names. If a name was not found in the FundRef registry, it may not be the canonical name form, it may be a program name rather than an organization name, or it may be an organization not yet included in FundRef Registry. If you know of another name form or a parent organization name for a “not found” item on this list below, please share that information.

FundRef Name	FundRef Organization Name
U.S. Department of the Interior (DOI)	U.S. Department of the Interior
National Science Foundation (NSF)	National Science Foundation

Geophysical Research Letters

RESEARCH LETTER

10.1029/2020GL087862

Key Points:

- SLR increases sediment deposition on the marsh platform but reduces the sediment-trapping capacity of tidal flats and bays
- For a given SLR the increase of bottom sediments resuspended and exported out of the system is more significant for sand than mud fraction
- Landforms lower with respect to the tidal frame are more affected by SLR than salt marshes

Supporting Information:

- Supporting Information S1

Correspondence to:

X. Zhang,
zhangbu@bu.edu

Citation:

Zhang, X., Leonardi, N., Donatelli, C., & Fagherazzi, S. (2020). Divergence of sediment fluxes triggered by sea-level rise will reshape coastal bays. *Geophysical Research Letters*, 47, e2020GL087862. <https://doi.org/10.1029/2020GL087862>

Received 6 MAR 2020

Accepted 17 MAY 2020

Accepted article online 30 MAY 2020

Divergence of Sediment Fluxes Triggered by Sea-Level Rise Will Reshape Coastal Bays

Xiaohe Zhang¹ , Nicoletta Leonardi² , Carmine Donatelli² , and Sergio Fagherazzi¹ 

¹Department of Earth and Environment, Boston University, Boston, MA, USA, ²Department of Geography and Planning, University of Liverpool, Liverpool, UK

Abstract Sediment budget and sediment availability are direct metrics for evaluating the resilience of coastal bays to sea-level rise (SLR). Here we use a high-resolution numerical model of a tidally dominated marsh-lagoon system to explore feedbacks between SLR and sediment dynamics. SLR augments tidal prism and inundation depth, facilitating sediment deposition on the marsh platform. At the same time, our results indicate that SLR enhances ebb-dominated currents and increases sediment resuspension, reducing the sediment-trapping capacity of tidal flats and bays and leading to a negative sediment budget for the entire system. This bimodal distribution of sediments budget trajectories will have a profound impact on the morphology of coastal bays, increasing the difference in elevation between salt marshes and tidal flats and potentially affecting intertidal ecosystems. Our results also clearly indicate that landforms lower with respect to the tidal frame are more affected by SLR than salt marshes.

1. Introduction

Coastal bays are ecologically and commercially valuable areas located at the interface of land and ocean. Shallow coastal bays are typically composed of salt marshes and tidal flats (Fagherazzi et al., 2012; Redfield, 1972). Salt marshes support biodiversity, improve water quality by filtering nutrients and pollutants, mitigate river floods, protect against storm damage, and sequester carbon in the soil (Alizad et al., 2018; Ganju et al., 2017; Kirwan et al., 2016; Morris et al., 2002). Tidal flats provide stopover and breeding habitats for birds, dissipate wave energy, and are commercially important for the shellfish industry (Murray et al., 2019).

The location of coastal bays makes them vulnerable and sensitive to sea-level rise (SLR) (Stevenson et al., 1986). Complex interplay between rivers, tides, and waves control sediment fluxes in a bay and drive its long-term evolution. For instance, reduced sediment supply is considered as the main factor causing marsh deterioration and erosion of bay substrate in the Mississippi River delta (Reed, 1995; Syvitski et al., 2009). Similarly, sediment loss has changed the morphology of the Venice Lagoon, Italy, and San Pablo Bay, USA, deepening tidal flats and reducing the network of tidal channels (Carniello et al., 2009; Jaffe et al., 2007). Predicting the morphological response of coastal systems to SLR is crucial, because of the alarming global SLR projections with a maximum scenario reaching 2 m by 2100 (Parris et al., 2012; Ranger et al., 2013; Sweet et al., 2017). Determining whether coastal bays are stable and in equilibrium under SLR requires the quantification of sediment fluxes, and in particular the exchange of material between different geomorphic units like tidal flats and salt marshes (Duvall et al., 2019; French, 2006; Lacy et al., 2019). Sediment inputs are required to accrete tidal flats and salt marshes in addition to organic matter contribution and maintain constant water depths in a period of accelerated SLR (Horton et al., 2018; Schuerch et al., 2019).

Previous process-based studies showed that SLR could gradually reduce the intertidal area of bays and lead to severe incision, especially in deeper channels (Alizad et al., 2016; Elmilady et al., 2019; FitzGerald et al., 2008; Ganju & Schoellhamer, 2010; Zhou et al., 2013). In San Pablo Bay and Suisun Bay, California, USA, while SLR may initially increase sediment retention and deposition because of reduced wave erosion due to an increase in water depth, limited sediment supply would eventually lead to erosion. While informative, process-based studies typically utilize long-term morphological numerical simulations whose spatial resolution is too coarse to capture potential differences in salt marsh and tidal flat response to SLR observed in field studies (Allen, 2000; Cahoon et al., 2006; Kirwan et al., 2016; Redfield, 1972). In order to more

accurately predict future changes in the morphology and ecosystem functioning of coastal bays, future modeling efforts need to account for these different responses.

To better understand the resilience of salt marshes to SLR, a number of studies have utilized coupled geomorphological/ecological models which assume a marsh accretion rate proportional to the inundation period and a suspended sediment concentration (SSC) spatially uniform (Belliard et al., 2016; D'Alpaos et al., 2011; Donatelli, Ganju, Fagherazzi, et al., 2018; Donatelli, Ganju, Zhang, et al., 2018; Kirwan et al., 2010; Mariotti & Fagherazzi, 2012). These models represent a step forward; however, they have a limited ability to accurately predict the response to SLR since they neglect the complex sediment dynamics between marsh surfaces and tidal flats and devote little attention to addressing the stability of physically connected tidal flats, crucial for understanding the response of the coastal bay system.

SLR affects hydrodynamic and sediment fluxes in coastal bays, ultimately determining the trapping capacity of sediments on tidal flats and marsh platforms and the sediment budget of the entire systems; yet these dynamics are not fully understood. To fill this gap, we use a high-resolution numerical model (Delft3D) of Plum Island Sound, MA (USA), a tidally and marsh dominated system. We couple a vegetation module to hydrodynamics and sediment transport to study the influence of different SLR scenarios on tidal flows, bottom erosion, resuspension of bed sediments, and trapping capacity of cohesive and non-cohesive sediments within the entire system. Our quantitative approach is general and can be used as a template to determine the response of any coastal bay to SLR.

2. Study Site

Plum Island Sound (Figure 1a) is a tidally dominated bay characterized by expansive salt marshes. The bay is located along the northeastern shoreline of Massachusetts, USA, and it covers an area of about 59.8 km² with more than 60% dominated by *Spartina alterniflora* and *Spartina patens* marshes (Figure 1d). The narrow sound extends approximately 12 km in the north-south direction and receives waters from three distinct fluvial watersheds: the Parker, Rowley, and Ipswich Rivers. The tide is semidiurnal with mean tidal range of 2.6 m. The mean depth of the sound is 3.0 m with a maximum depth of about 10 m at the inlet (Figure 1c). Wind waves act mainly on shallow tidal shoals (<1 m), and the induced shear stresses are 1 order of magnitude smaller than those due to tides (Fagherazzi et al., 2014). The total monthly freshwater discharge of the three rivers ranges from 1.40 to 15.4 m³·s⁻¹ but is negligible compared to the tidal prism (approximately 6.37 × 10⁷ m³ in a spring tide, Zhang et al., 2019). The bed composition is a mixture of mud (0–63 μm), very fine sand (63–125 μm), fine sand (125–250 μm), and medium sand (250–500 μm), with more mud in tidal flats along the marsh boundaries and more sand in the sound (Fagherazzi et al., 2014, Figure 1e). Since riverine sediments provide less than 10% of the necessary volume, maintaining marsh elevation close to the high tide mark will require significant supply from tidal flats and oceanic sources (Hopkinson et al., 2018). The rate of SLR is about 2.8 mm·yr⁻¹ in this region (Claessens et al., 2006), and sea level has increased by 0.3–0.5 m from 1921 to 2015 (Figure 1b).

3. Methods

3.1. Model Setup

Hydrodynamics and sediment transport were simulated using a high-resolution (20 m × 20 m) 2-D Delft3D FLOW/MOR model (Lesser et al., 2004), incorporating a 2-D vegetation module (Baptist, 2005; Horstman et al., 2013; Temmerman et al., 2005). The domain consists of 703 × 410 grid cells with three river inputs and three ocean open boundaries (supporting information Figure S1). The resolution of the mesh is sufficient to capture the main tidal channels and the propagation of the tide in the system (Zhang et al., 2019). The daily riverine discharges prescribed at the river boundaries were 1 m³·s⁻¹ for the Parker River, 0.2 m³·s⁻¹ for the Rowley River, and 5 m³·s⁻¹ for the Ipswich River. Tidal forcing at the three open ocean boundaries employed modified tidal harmonics generated from the large-scale ADCIRC model of the Atlantic Coast (Szpilka et al., 2016, Table S1). Compared to four observation sites across the system, the model accuracy has an error in harmonic amplitude less than 5 cm and in phase less than 5° (Figures 1a and S2).

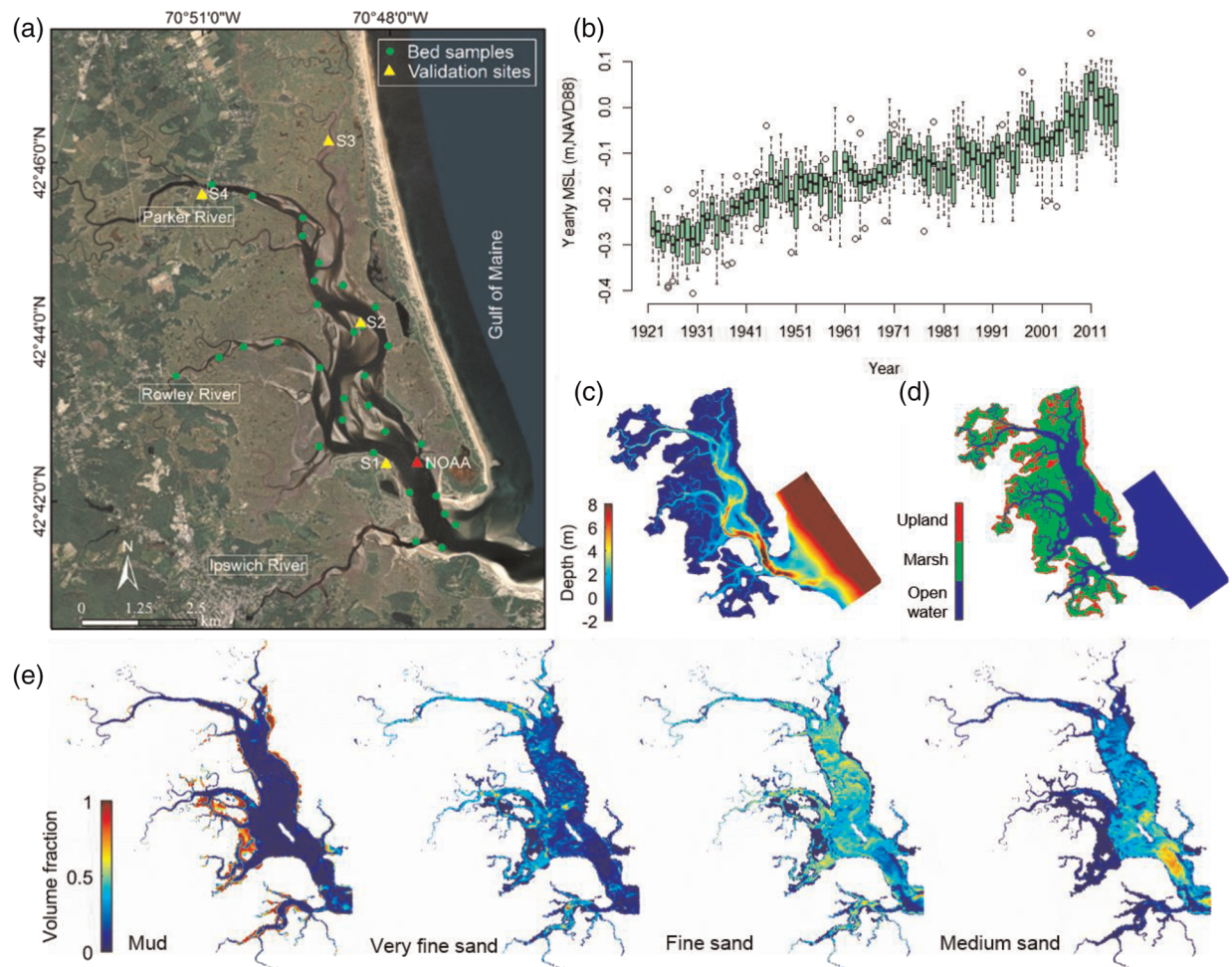


Figure 1. (a) Locations of Plum Island Sound, bed samples, and validation sites. S1 tidal station is at Ipswich Bay Yacht Club pier; S4 tidal station is in the Parker River near Route 1A Bridge. S2 and S3 are ADCP measurement sites in 2010 and 2017, respectively. The NOAA station 8441241 is indicated with a red triangle; (b) mean sea level recorded at NOAA station 8443970; (c) water depth; and (d) spatial distribution of upland, marsh, and open water. (e) Initial bottom conditions: Volume fractions of four sediment classes obtained from a combination of field data and numerical simulations.

The topography was obtained from a combination of Lidar-derived digital elevation models and GPS bathymetric measurements. The error in the elevation of the salt marshes was deemed acceptable (Alizad et al., 2020). Details on bed roughness and representative vegetation parameters used in the simulations can be found in Zhang et al. (2019). Properties of the cohesive sediment class and three non-cohesive sediment classes employed in model experiments were based on bed samples and field resuspension experiments (Tables S2 and S3 and Figure S6). Following Van der Wegen et al. (2011), we implemented numerical simulations to generate a synthetic bed composition (supporting information Part 2), to be used as the initial bottom condition (Figure 1e). Optimized parallel computing resources were tested to enable full morphological simulations with a high-spatial resolution (Table S5).

3.2. Model Experiments

Three different sets of experiments were undertaken to understand how SLR would alter coastal bay environments and their habitats. The series of experiments are described below:

Experiment 1: *Initial SSC = 30 mg/L, fixed sediment bed.* These simulations allow sediment in the water column to settle to the bed and be resuspended. By imposing a fixed bed, we can investigate the fate of new material entering the system via the water column and determine what proportion of material is retained by the different coastal bay environments under each SLR scenario. Six SLR scenarios were employed, Sea Level = MSL, MSL + 0.1 m, MSL + 0.2 m,

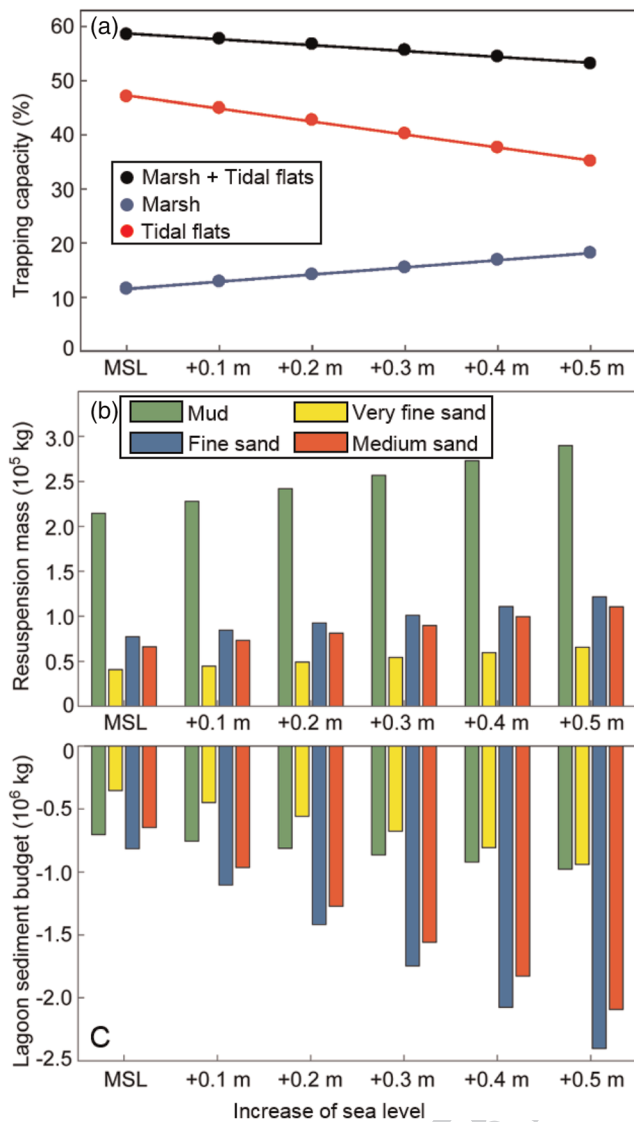


Figure 2. (a) Trapping capacity of suspended sediments on the marsh platform, tidal flats (including also tidal channels), and entire bay (lagoon) system (marsh + tidal flats) under different SLR scenarios. The trapping capacity is the percent of initially released sediments in the water column deposited in different parts of the system. The amount of resuspended sediments (b) and sediment budget within the lagoon (c) averaged in two spring tidal cycles for different bed compositions: Mud, very fine sand, fine sand, and medium sand for five SLR scenarios. Negative values (c) indicate sediments escaping the lagoon.

increases with SLR, while that in the tidal flats decreases. The total sediment captured by the system decreases as sea level increases. A SLR of 0.5 m leads to 6.6% more sediment deposited on the marsh platform, 12.1% less sediment is trapped in the tidal flats, and a loss of 5.5% for the entire system (Figure 2a).

In the second set of experiments, results show that more bottom sediments are resuspended into the water column as sea level increases (Figure 2b). A SLR of 0.5 m leads to 35% more mud resuspended into the water column, and an increase of 60%, 58%, and 68% for very fine sand, fine sand, and medium sand, respectively. Some of these resuspended sediments then flushed out the bay by ebb tides. The retention capacity of autochthonous sediments in the system is reduced by 39% for mud, and by 166%, 195%, and 223% for the three sand classes (Figure 2c).

MSL + 0.3 m, MSL + 0.4 m, and MSL + 0.5 m. Experiment 1 simulations were ran for two spring neap tidal cycles (30 days).

Experiment 2: *Initial SSC = 0 mg/L, active sediment bed.* In these experiments, we investigate resuspension, transport, and fate of sediment originating from the bed under the six different SLR scenarios previously employed. To this end we used the sediment bed with variable composition detailed in section 3.1 and associated supporting information (Tables S2 and S3 and Figures 1e, S4, and S5). Initial SSC was set to 0 mg/L to ensure that all material transported can be attributed to resuspension from the sediment bed. For these experiments, it was assumed that the bed morphology was the same at the beginning of each SLR scenario. In this way, potential changes in bed morphology are ignored. Experiment 2 simulations ran for a single spring neap tidal cycle (15 days).

Experiment 3: *Incremental sea level, dynamic morphological response.* To better mimic the process of a gradually increasing sea level, we conducted full long-term morphological simulations of 25 years applying a morphological factor (MF) of 50, with sea level at the ocean boundary increasing linearly by 2 cm·yr⁻¹, for a total of 50 cm (Figure 4). The rate of SLR applied reflects high-end projections of 2 m by 2100 (Church et al., 2013; Parris et al., 2012; Ranger et al., 2013; Vermeer & Rahmstorf, 2009). Simulation time was limited to 25 years since higher-resolution models are typically affected by cumulative errors (Ranasinghe et al., 2011). We designed an extra control experiment with the same setup as in Experiment 3 but with a fixed bed, to evaluate the potential effect of morphological changes on sediment remobilization and trapping within the lagoon.

Analysis of spatial erosion and deposition patterns, tidal flow, and tidal asymmetry for the various simulations and SLR scenarios were undertaken to determine the physical mechanisms affecting sediment budgets in the whole coastal bay system and within the different coastal bay environments.

4. Results

To quantitatively evaluate sediment dynamics within the estuary, we separate the system into marsh platform, tidal flats (including also tidal channels, Figure 1d), and shelf. The first set of experiments show that the trapping capacity of allocthonous sediment on the marsh platform

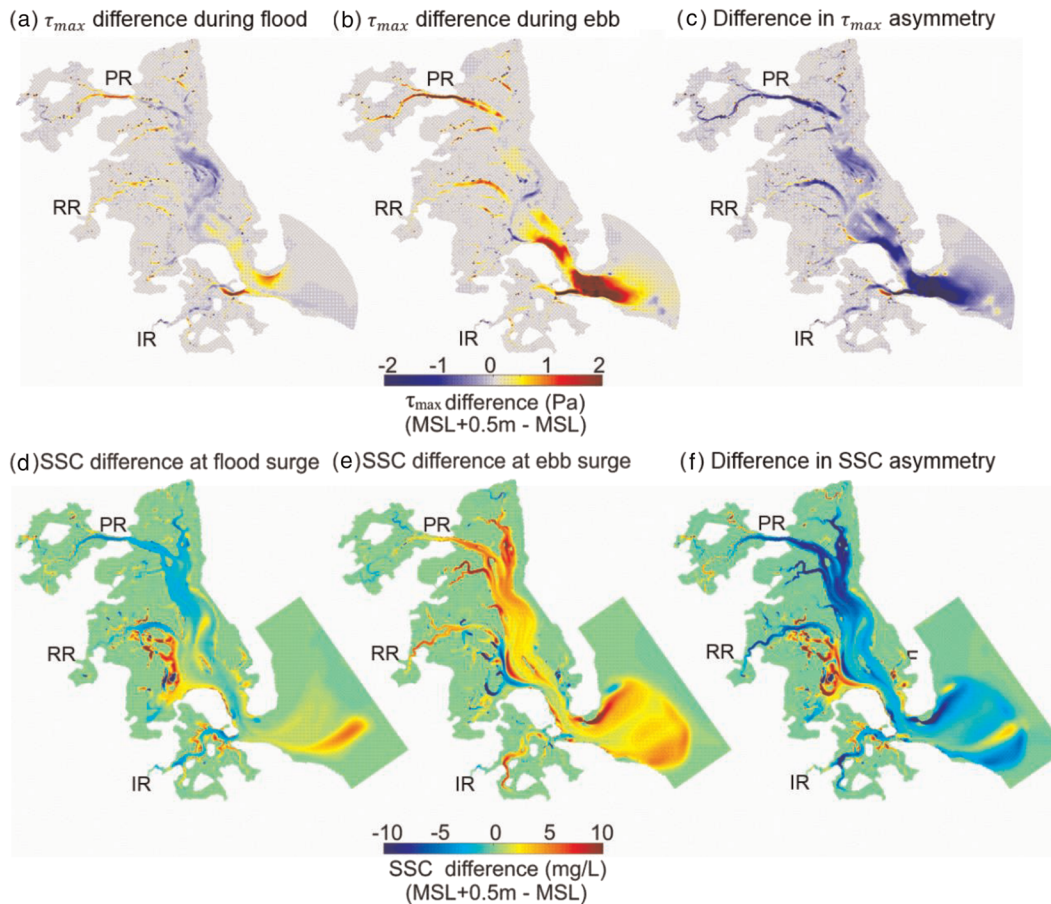


Figure 3. Difference in key parameters between the MSL + 0.5 m scenario and the MSL scenario. PR, RR, and IR indicate locations of the Parker, Rowley, and Ipswich Rivers, respectively. Change in maximum shear stress for a spring tide cycle, during flood (a) and ebb (b), where positive values depict an increase due to SLR. Change in maximum shear stress asymmetry (flood-ebb) where negative values indicate a reduction in flood dominance due to SLR (c). Change in SSC for the mud fraction at flood surge (d) and ebb surge (e). Change in SSC asymmetry (flood-ebb) (f).

Tidal flows within the sound become more ebb dominated with SLR (Figures 3a–3c and S8); correspondingly, more bottom sediments are resuspended during ebb than during flood for all sediment classes (Figures 3, S9, and S10). During flood, SLR decreases the SSC of mud in the Parker River and in the upper sound while SSC increases in the lower sound, especially in the area bordering the Rowley River (Figure 3d). During ebb more mud is suspended in the water column in the tidal flats and rivers (Figure 3e), favoring sediment export outside the sound. This SSC asymmetry is even more obvious for sand fractions (Figures S9 and S10).

After a 25-year-long morphological simulation with a 0.5-m total increase in sea level, intensive incision occurred in the lower sound and in the deep channels, while areas bordering marsh edges accreted (Figures 4a–4c). The yearly increase in sea level ($2 \text{ cm}\cdot\text{yr}^{-1}$) led to increased deposition of fine-grain sediments on the marsh, relative to present-day deposition (Figure 4d). At the same time, the sediment budget for the entire system decreased, with total erosion an order of magnitude larger than deposition on the marsh (Figure 4e). By keeping the bed fixed, the total amount of sediment exported out of the system after 25 years was reduced by about 50%.

Variations in tidal asymmetry within the sound may also affect sediment transport and the trapping capacity of the entire system (Friedrichs & Aubrey, 1988; Van der Wegen, 2013). However, the change of M4/M2 amplitude ratio is small (Figure S7, Pawlowicz et al., 2002). The ocean inlet, lower sound, and Parker River experience higher flow shear stresses during ebb when sea level increases (Figure 3), while the increase of maximum shear stress during the flood period is very limited (Figure S8). Sediment budget

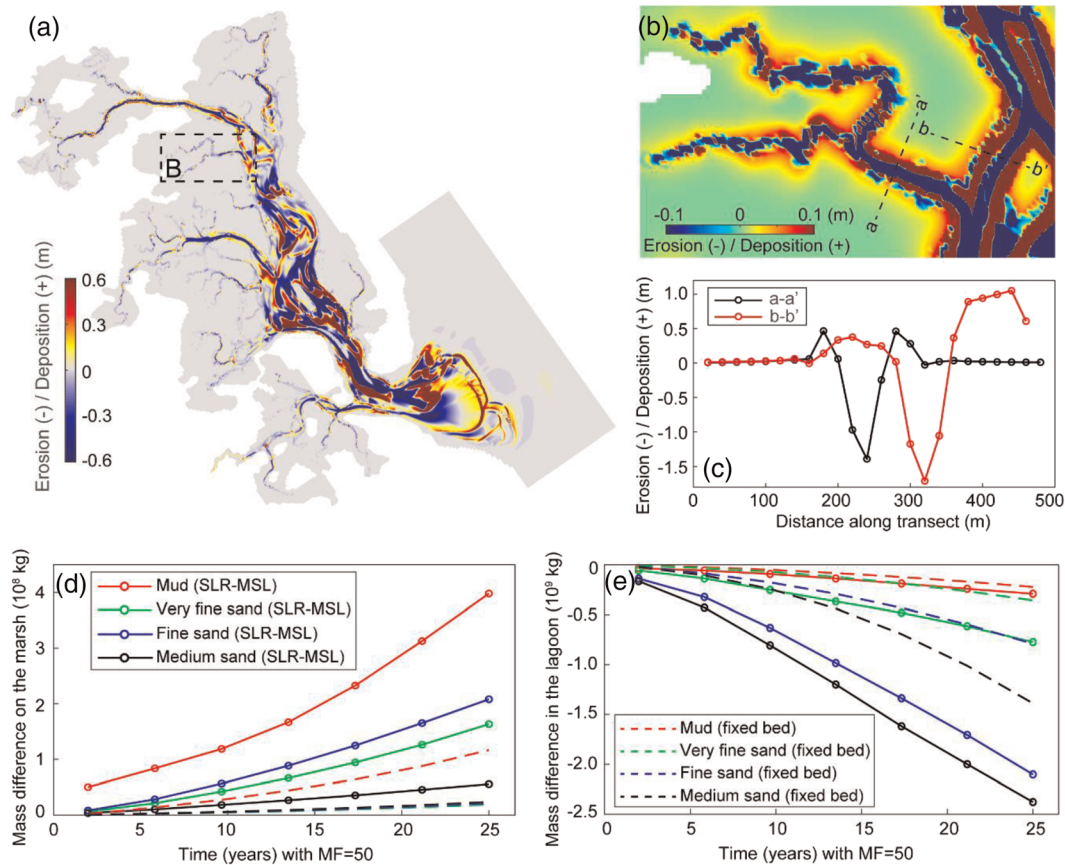


Figure 4. Sediment deposition and erosion patterns for the 25-year MSL + 2 cm·yr⁻¹ morphological simulation (SLR scenario) compared against the 25-year MSL + 0 cm·yr⁻¹ morphological simulation (no SLR scenario). Change in bed thickness at the end of the 25-year simulations (SLR scenario-no SLR scenario) where deposition indicates increased bed thickness (a). Change in bed thickness in zoomed area (b) and along two transects (a-a', b-b') across the marsh platform and channels (c). Difference in sediment deposition for four sediment size classes averaged over spring neap tidal cycles, on the marsh platform (d), and inside the lagoon (e) over time (SLR scenario-no SLR scenario). Dash lines in (d) and (e) are results with a fixed bed (no morphological change).

depends not only on the magnitude of bottom shear stresses but also on the time interval during which flow shear stresses exceed the critical shear stress for erosion within one tidal cycle (Figure S11). The longer this period, the more time the tide has to export material out of the system. SLR of 0.5 m extended by more than 20% the time period during which bottom shear stress exceeds the critical shear stress for mud ($\tau = 0.1 \text{ N}\cdot\text{m}^{-2}$) (Figure S6, Kalnejais et al., 2010) and the critical shear stress for medium sand ($\tau = 0.21 \text{ N}\cdot\text{m}^{-2}$) (Figure S11, Van Rijn, 1993). While this allowed more sediment to flush out of the system during ebb cycles, an increase in resuspension of the mud fraction during flood cycles contributed to increased deposition of this sediment fraction on the marsh platform in response to higher sea levels.

5. Discussion

Plum Island Sound is a typical shallow bay consisting of salt marshes and tidal flats and is therefore an ideal place to test the effect of SLR on sediment budgets utilizing high-resolution (20 m) numerical simulations. Although our morphological simulations are limited to several decades, our results captured the variability of sediment deposition across the system in response to SLR. This is exemplified by the increase in sediment deposition on marsh platforms and increased sediment erosion in the tidal flats within the shallow bay.

SLR caused higher bottom shear stresses during ebb cycles, most prominently seen in deep channels and the lower sound, and an overall shift toward ebb-dominant tidal currents. These results are in agreement with hydrodynamic simulations in the Ria Formosa lagoon along the Portuguese coast (Carrasco et al., 2018), where peak-flood velocities on the marsh platform slightly increase tidal currents, and the main inlet

becomes less flood dominant with SLR. In the Virginia Coast Reserve, USA, Mariotti et al. (2010) showed that SLR would lead to resuspension and subsequent scour of lagoon beds due to higher bottom shear stress during a tidal cycle. Our simulations also show that higher bottom shear stresses during ebb resuspend more sediments into the water column, favoring the export of material out of the sound, and thus reducing the sediment stock of the system.

Several tidal flats are eroded because of an increase in sea level (Figure 4a). A larger tidal prism triggered by SLR augments velocities and bottom shear stresses, resuspending sediment from tidal flats. A similar mechanism was also observed by Donatelli, Ganju, Zhang, et al. (2018); in their simulations the deterioration of salt marshes resulted in an increase of tidal prism and the erosion of tidal flats, reducing the stock of material available for long-term marsh accretion. Our results further show that with dynamic morphological simulations the flux of sediment out of the bay is larger with respect to simulations using a fixed bed (Figure 4e). This is because the erosion of intertidal flats increases the tidal prism, promoting further erosion. This positive feedback could remove large volumes of sediment from the bay, possibly jeopardizing important sources of material for the salt marshes.

Interestingly, the increase of bottom sediment flux out of the system in response to higher sea levels is more significant for the sand fraction than for the mud fraction. This is because flood currents under higher sea levels are sufficient to resuspend mud, but not sand, from the sound bed, transporting it onto the marsh platform where the mud deposits and is retained (Zhang et al., 2019). In contrast, only ebb currents are fast enough to erode the sand and transport it to the ocean. Marshes therefore act as a storage area for fine sediments during higher sea level conditions (Figure 4a). The different behavior of mud and sand fractions is a mechanism which may allow salt marshes to keep pace with SLR. This sorting process has been observed in the microtidal Great Sippewissett Marsh, MA, USA, where the entire mud fraction at the bottom was almost completely replaced with sand between 1979 and 2015 (Valiela et al., 2018). In a mesotidal system in Southeastern Essex, England, it was observed that fine-grain sediments eroded from the marsh edge are responsible for marsh accretion on the platform in response to SLR (Reed, 1988). Sediment coarsening at the delta front was observed in the Yangtze Delta, China, where erosion provided sediments to sustain salt marshes despite increasing sea levels and reduced riverine sediment loads in the last half century (Yang et al., 2018, 2020).

While the results of this study are based on only one bay, the key conclusions are of general validity: An increase in water level favors sediment storage in salt marshes if sediment is available, while an increase in tidal prism and related tidal currents triggers erosion of bottom sediments in tidal flats and channels. The erosion of bay beds may affect both ecosystem functioning and geomorphic stability. Increased water depth and SSC in the bay can affect light availability and therefore benthic primary production and the growth of submerged aquatic vegetation (Lawson et al., 2007). The increased tidal inundation would also decrease the periods during which tidal flats are subaerial, threatening habitats for birds and shellfish (Field et al., 2017). Because of SLR, wind waves might lead to more erosion at marsh edges. First because increased water depths reduce wave energy dissipation within the bay (Li et al., 2019; Mariotti et al., 2010); second the bimodal geomorphic change explored herein would increase the height of the marsh scarp, making it more vulnerable to wave attack (Koppel et al., 2004).

The lack of information on inner-shelf bottom data and the absence of processes that resuspend these sediments and transport them in the sound is a limit of our study. Without accounting for the sediment import from the ocean, we cannot close the sediment budget for the entire system (Hopkinson et al., 2018). In many systems (e.g., Virginia, USA, and island of Sylt, Germany), it was found that intense storms can resuspend sediments along the shelf and transport them to shallow bays and salt marshes (Castagno et al., 2018; Lacy et al., 2019; Schuerch et al., 2012). The Labrador Current, Warm Core Rings, and the Gulf Stream can also affect the along shelf transport and therefore the marine fluxes of sediment in Plum Island Sound (Townsend et al., 2015; Zhang et al., 2016). Future research should evaluate the contribution of waves and shelf currents to sediment budgets under SLR.

Only high-spatial-resolution numerical models (tens of meters) can capture sediment dynamics between tidal flats, tidal creeks, and marsh platforms (Table S5). Many salt marsh modeling studies assume that the morphology does not change, while process-based morphological models in real systems (e.g., Western Scheldt, Suisun Bay, San Pablo Bay, and Yangtze Estuary) are generally too coarse to

capture dynamics between marshes, tidal flats, and tidal channels (Dam et al., 2016; Elmilady et al., 2019; Ganju & Schoellhamer, 2010; Zhou et al., 2013). Under SLR, the increased tidal prism can erode tidal flats, intensify ebb tidal flows, and further decrease sediment stocks. Ignoring these feedbacks caused by morphological changes in salt marsh models would lead to an overestimation of sediment trapping in bay systems.

6. Conclusion

SLR can directly affect hydrodynamics, sediment transport, and morphological stability of coastal bays. Tidal flats and salt marshes behave differently in terms of sediment budget and trapping capacity after an increase in sea level. SLR facilitates sediment deposition on the marsh platform due to an increase in inundation depth and hydroperiod. Within the connected shallow bay, SLR enhances erosion of tidal flats and tidal channels via ebb-dominated currents and reduces the sediment-trapping capacity of bay beds, leading to a negative sediment budget for the entire system. Our results therefore indicate that landforms lower in the tidal frame are more affected by SLR and will experience more change in the future. With a worldwide decrease in riverine sediment loads caused by anthropogenic perturbations, a net export of sediment from coastal bays triggered by SLR will further compromise the coastline morphology. SLR is likely to reshape coastal bays and therefore affect their delicate ecosystems.

Data Availability Statement

The topography data are provided by LTER-PIE (<https://pie-lter.ecosystems.mbl.edu/data>). Simulations are available at the website (<http://doi.org/10.5281/zenodo.3360873>).

Acknowledgments

This research is funded by the USA National Science Foundation (NSF) Awards 1637630 (PIE LTER) and 1832221 (VCR LTER), the U.S. Department of the Interior (DOI) Hurricane Sandy Recovery Program ID G16AC00455.

References

- Alizad, K., Hagen, S. C., Medeiros, S. C., Bilskie, M. V., Morris, J. T., Balthis, L., & Buckel, C. A. (2018). Dynamic responses and implications to coastal wetlands and the surrounding regions under sea level rise. *PLoS ONE*, *13*(10), e0205176. <https://doi.org/10.1371/journal.pone.0205176>
- Alizad, K., Hagen, S. C., Morris, J. T., Medeiros, S. C., Bilskie, M. V., & Weishampel, J. F. (2016). Coastal wetland response to sea-level rise in a fluvial estuarine system. *Earth's Future*, *4*, 483–497. <https://doi.org/10.1002/2016EF000385>
- Alizad, K., Medeiros, S. C., Foster-Martinez, M. R., & Hagen, S. C. (2020). Model sensitivity to topographic uncertainty in meso- and microtidal marshes. *IEEE Journal of Selected Topics in Applied Earth Observations and Remote Sensing*, *13*, 807–814. <https://doi.org/10.1109/JSTARS.2020.2973490>
- Allen, J. R. (2000). Morphodynamics of Holocene salt marshes: A review sketch from the Atlantic and Southern North Sea coasts of Europe. *Quaternary Science Reviews*, *19*(12), 1155–1231. [https://doi.org/10.1016/S0277-3791\(99\)00034-7](https://doi.org/10.1016/S0277-3791(99)00034-7)
- Baptist, M. J. (2005). *Modelling floodplain biogeomorphology*. TU Delft: Delft University of Technology.
- Belliard, J. P., Di Marco, N., Carniello, L., & Toffolon, M. (2016). Sediment and vegetation spatial dynamics facing sea-level rise in microtidal salt marshes: Insights from an ecogeomorphic model. *Advances in Water Resources*, *93*, 249–264. <https://doi.org/10.1016/j.advwatres.2015.11.020>
- Cahoon, D. R., Hensel, P. F., Spencer, T., Reed, D. J., McKee, K. L., & Saintilan, N. (2006). Coastal wetland vulnerability to relative sea-level rise: Wetland elevation trends and process controls. In *Wetlands and natural resource management*, (pp. 271–292). Berlin, Heidelberg: Springer.
- Carniello, L., Defina, A., & D'Alpaos, L. (2009). Morphological evolution of the Venice lagoon: Evidence from the past and trend for the future. *Journal of Geophysical Research*, *114*, F04002. <https://doi.org/10.1029/2008JF001157>
- Carrasco, A. R., Plomaritis, T., Reynolds, J., Ferreira, Ó., & Roelvink, D. (2018). Tide circulation patterns in a coastal lagoon under sea-level rise. *Ocean Dynamics*, *68*(9), 1121–1139. <https://doi.org/10.1007/s10236-018-1178-0>
- Castagno, K. A., Jiménez-Robles, A. M., Donnelly, J. P., Wiberg, P. L., Fenster, M. S., & Fagherazzi, S. (2018). Intense storms increase the stability of tidal bays. *Geophysical Research Letters*, *45*, 5491–5500. <https://doi.org/10.1029/2018GL078208>
- Church, J. A., Clark, P. U., Cazenave, A., Gregory, J. M., Jevrejeva, S., Levermann, A., & Payne, A. J. (2013). Sea-level rise by 2100. *Science*, *342*(6165), 1445–1445. <https://doi.org/10.1126/science.342.6165.1445-a>
- Claessens, L., Hopkinson, C., Rastetter, E., & Vallino, J. (2006). Effect of historical changes in land use and climate on the water budget of an urbanizing watershed. *Water Resources Research*, *42*, W03426. <https://doi.org/10.1029/2005WR004131>
- D'Alpaos, A., Mudd, S. M., & Carniello, L. (2011). Dynamic response of marshes to perturbations in suspended sediment concentrations and rates of relative sea level rise. *Journal of Geophysical Research*, *116*, F04020. <https://doi.org/10.1029/2011JF002093>
- Dam, G., Van der Wegen, M., Labeur, R. J., & Roelvink, D. (2016). Modeling centuries of estuarine morphodynamics in the Western Scheldt estuary. *Geophysical Research Letters*, *43*, 3839–3847. <https://doi.org/10.1002/2015GL066725>
- Donatelli, C., Ganju, N. K., Fagherazzi, S., & Leonardi, N. (2018). Seagrass impact on sediment exchange between tidal flats and salt marsh, and the sediment budget of shallow bays. *Geophysical Research Letters*, *45*, 4933–4943. <https://doi.org/10.1029/2018GL078056>
- Donatelli, C., Ganju, N. K., Zhang, X., Fagherazzi, S., & Leonardi, N. (2018). Salt marsh loss affects tides and the sediment budget in shallow bays. *Journal of Geophysical Research: Earth Surface*, *123*, 2647–2662. <https://doi.org/10.1029/2018JF004617>
- Duvall, M. S., Wiberg, P. L., & Kirwan, M. L. (2019). Controls on sediment suspension, flux, and marsh deposition near a bay-marsh boundary. *Estuaries and Coasts*, *42*(2), 403–424. <https://doi.org/10.1007/s12237-018-0478-4>
- Elmilady, H., van der Wegen, M., Roelvink, D., & Jaffe, B. E. (2019). Intertidal area disappears under sea level rise: 250 years of morphodynamic modeling in San Pablo Bay, California. *Journal of Geophysical Research: Earth Surface*, *124*, 38–59.

- Fagherazzi, S., Kirwan, M. L., Mudd, S. M., Guntenspergen, G. R., Temmerman, S., D'Alpaos, A., & Clough, J. (2012). Numerical models of salt marsh evolution: Ecological, geomorphic, and climatic factors. *Reviews of Geophysics*, 50, RG1002. <https://doi.org/10.1029/2011RG000359>
- Fagherazzi, S., Mariotti, G., Banks, A. T., Morgan, E. J., & Fulweiler, R. W. (2014). The relationships among hydrodynamics, sediment distribution, and chlorophyll in a mesotidal estuary. *Estuarine, Coastal and Shelf Science*, 144, 54–64. <https://doi.org/10.1016/j.ecss.2014.04.003>
- Field, C. R., Bayard, T. S., Gjerdrum, C., Hill, J. M., Meiman, S., & Elphick, C. S. (2017). High-resolution tide projections reveal extinction threshold in response to sea-level rise. *Global Change Biology*, 23(5), 2058–2070. <https://doi.org/10.1111/gcb.13519>
- FitzGerald, D. M., Fenster, M. S., Argow, B. A., & Buynevich, I. V. (2008). Coastal impacts due to sea-level rise. *Annual Review of Earth and Planetary Sciences*, 36(1), 601–647. <https://doi.org/10.1146/annurev.earth.35.031306.140139>
- French, J. (2006). Tidal marsh sedimentation and resilience to environmental change: Exploratory modelling of tidal, sea level and sediment supply forcing in predominantly allochthonous systems. *Marine Geology*, 235(1–4), 119–136. <https://doi.org/10.1016/j.margeo.2006.10.009>
- Friedrichs, C. T., & Aubrey, D. G. (1988). Non-linear tidal distortion in shallow well-mixed estuaries: A synthesis. *Estuarine, Coastal and Shelf Science*, 27(5), 521–545. [https://doi.org/10.1016/0272-7714\(88\)90082-0](https://doi.org/10.1016/0272-7714(88)90082-0)
- Ganju, N. K., Defne, Z., Kirwan, M. L., Fagherazzi, S., D'Alpaos, A., & Carniello, L. (2017). Spatially integrative metrics reveal hidden vulnerability of microtidal salt marshes. *Nature Communications*, 8(1), 14,156. <https://doi.org/10.1038/ncomms14156>
- Ganju, N. K., & Schoellhamer, D. H. (2010). Decadal-timescale estuarine geomorphic change under future scenarios of climate and sediment supply. *Estuaries and Coasts*, 33(1), 15–29. <https://doi.org/10.1007/s12237-009-9244-y>
- Hopkinson, C. S., Morris, J. T., Fagherazzi, S., Wollheim, W. M., & Raymond, P. A. (2018). Lateral marsh edge erosion as a source of sediments for vertical marsh accretion. *Journal of Geophysical Research: Biogeosciences*, 123, 2444–2465. <https://doi.org/10.1029/2017JG004358>
- Horstman, E., Dohmen-Janssen, M., & Hulscher, S. J. M. H. (2013). Modeling tidal dynamics in a mangrove creek catchment in Delft3D. In *Coastal dynamics* (Vol. 2013, pp. 833–844). Q5 Q6
- Horton, B. P., Shennan, I., Bradley, S. L., Cahill, N., Kirwan, M., Kopp, R. E., & Shaw, T. A. (2018). Predicting marsh vulnerability to sea-level rise using Holocene relative sea-level data. *Nature Communications*, 9(1), 2687. <https://doi.org/10.1038/s41467-018-05080-0> Q7
- Jaffe, B. E., Smith, R. E., & Foxgrover, A. C. (2007). Anthropogenic influence on sedimentation and intertidal mudflat change in San Pablo Bay, California: 1856–1983. *Estuarine, Coastal and Shelf Science*, 73(1–2), 175–187.
- Kalnejais, L. H., Martin, W. R., & Bothner, M. H. (2010). The release of dissolved nutrients and metals from coastal sediments due to resuspension. *Marine Chemistry*, 121(1–4), 224–235. <https://doi.org/10.1016/j.marchem.2010.05.002>
- Kirwan, M. L., Guntenspergen, G. R., d'Alpaos, A., Morris, J. T., Mudd, S. M., & Temmerman, S. (2010). Limits on the adaptability of coastal marshes to rising sea level. *Geophysical Research Letters*, 37, L23401. <https://doi.org/10.1029/2010GL045489>
- Kirwan, M. L., Temmerman, S., Skeeahan, E. E., Guntenspergen, G. R., & Fagherazzi, S. (2016). Overestimation of marsh vulnerability to sea level rise. *Nature Climate Change*, 6(3), 253–260. <https://doi.org/10.1038/nclimate2909>
- Koppel, J. V. D., Wal, D. V. D., Bakker, J. P., & Herman, P. M. (2004). Self-organization and vegetation collapse in salt marsh ecosystems. *The American Naturalist*, 165(1), E1–E12.
- Lacy, J. R., Foster-Martinez, M. R., Allen, R. M., Ferner, M. C., & Callaway, J. C. (2019). Seasonal variation in sediment delivery across the bay marsh interface of an estuarine salt marsh. *Journal of Geophysical Research: Oceans*, 125. <https://doi.org/10.1029/2019JC015268> Q8
- Lawson, S. E., Wiberg, P. L., McGlathery, K. J., & Fugate, D. C. (2007). Wind-driven sediment suspension controls light availability in a shallow coastal lagoon. *Estuaries and Coasts*, 30(1), 102–112. <https://doi.org/10.1007/BF02782971>
- Lesser, G. R., Roelvink, J. V., Van Kester, J. A. T. M., & Stelling, G. S. (2004). Development and validation of a three-dimensional morphological model. *Coastal Engineering*, 51(8–9), 883–915. <https://doi.org/10.1016/j.coastaleng.2004.07.014>
- Li, X., Leonardi, N., & Plater, A. J. (2019). Wave-driven sediment resuspension and salt marsh frontal erosion alter the export of sediments from macro-tidal estuaries. *Geomorphology*, 325, 17–28. <https://doi.org/10.1016/j.geomorph.2018.10.004>
- Mariotti, G., & Fagherazzi, S. (2012). Channels-tidal flat sediment exchange: The channel spillover mechanism. *Journal of Geophysical Research*, 117, C03032. <https://doi.org/10.1029/2011JC007378>
- Mariotti, G., Fagherazzi, S., Wiberg, P. L., McGlathery, K. J., Carniello, L., & Defina, A. (2010). Influence of storm surges and sea level on shallow tidal basin erosive processes. *Journal of Geophysical Research*, 115, C11012. <https://doi.org/10.1029/2009JC005892>
- Morris, J. T., Sundareshwar, P. V., Nietch, C. T., Kjerfve, B., & Cahoon, D. R. (2002). Responses of coastal wetlands to rising sea level. *Ecology*, 83(10), 2869–2877. [https://doi.org/10.1890/0012-9658\(2002\)083\[2869:ROCWTR\]2.0.CO;2](https://doi.org/10.1890/0012-9658(2002)083[2869:ROCWTR]2.0.CO;2)
- Murray, N. J., Phinn, S. R., DeWitt, M., Ferrari, R., Johnston, R., Lyons, M. B., & Fuller, R. A. (2019). The global distribution and trajectory of tidal flats. *Nature*, 565(7738), 222–225. <https://doi.org/10.1038/s41586-018-0805-8>
- Parris, A. S., P. Bromirski, V. Burkett, D. R. Cayan, M. E. Culver, J. H. Radley M. Horton et al. (2012). “Global sea level rise scenarios for the United States National Climate Assessment.”
- Pawlowicz, R., Beardsley, B., & Lentz, S. (2002). Classical tidal harmonic analysis including error estimates in MATLAB using T_TIDE. *Computers and Geosciences*, 28(8), 929–937. [https://doi.org/10.1016/S0098-3004\(02\)00013-4](https://doi.org/10.1016/S0098-3004(02)00013-4)
- Ranasinghe, R., Swinkels, C., Luijendijk, A., Roelvink, D., Bosboom, J., Stive, M., & Walstra, D. (2011). Morphodynamic upscaling with the MORFAC approach: Dependencies and sensitivities. *Coastal Engineering*, 58(8), 806–811. <https://doi.org/10.1016/j.coastaleng.2011.03.010>
- Ranger, N., Reeder, T., & Lowe, J. (2013). Addressing ‘deep’ uncertainty over long-term climate in major infrastructure projects: Four innovations of the Thames Estuary 2100 Project. *European Journal on Decision Processes*, 1(3–4), 233–262. <https://doi.org/10.1007/s40070-013-0014-5>
- Redfield, A. C. (1972). Development of a New England salt marsh. *Ecological Monographs*, 42(2), 201–237. <https://doi.org/10.2307/1942263>
- Reed, D. J. (1988). Sediment dynamics and deposition in a retreating coastal salt marsh. *Estuarine, Coastal and Shelf Science*, 26(1), 67–79. [https://doi.org/10.1016/0272-7714\(88\)90012-1](https://doi.org/10.1016/0272-7714(88)90012-1)
- Reed, D. J. (1995). The response of coastal marshes to sea-level rise: Survival or submergence? *Earth Surface Processes and Landforms*, 20(1), 39–48. <https://doi.org/10.1002/esp.3290200105>
- Schuerch, M., Rapaglia, J., Liebetrau, V., Vafeidis, A., & Reise, K. (2012). Salt marsh accretion and storm tide variation: An example from a barrier island in the North Sea. *Estuaries and Coasts*, 35(2), 486–500. <https://doi.org/10.1007/s12237-011-9461-z>
- Schuerch, M., Spencer, T., & Evans, B. (2019). Coupling between tidal mudflats and salt marshes affects marsh morphology. *Marine Geology*, 412, 95–106. <https://doi.org/10.1016/j.margeo.2019.03.008>

- Stevenson, J. C., Ward, L. G., & Kearney, M. S. (1986). Vertical accretion in marshes with varying rates of sea level rise. In *Estuarine variability*, (pp. 241–259). Academic Press.
- Sweet, W. V., Kopp, R. E., Weaver, C. P., Obeysekera, J., Horton, R. M., Thieler, E. R., & Zervas, C. (2017). Global and regional sea level rise scenarios for the United States.
- Syvitski, J. P., Kettner, A. J., Overeem, I., Hutton, E. W., Hannon, M. T., Brakenridge, G. R., & Nicholls, R. J. (2009). Sinking deltas due to human activities. *Nature Geoscience*, *2*(10), 681–686. <https://doi.org/10.1038/ngeo629>
- Szpilka, C., Dresback, K., Kolar, R., Feyen, J., & Wang, J. (2016). Improvements for the Western North Atlantic, Caribbean and Gulf of Mexico ADCIRC tidal database (EC2015). *Journal of Marine Science and Engineering*, *4*(4), 72. <https://doi.org/10.3390/jmse4040072>
- Temmerman, S., Bouma, T. J., Govers, G., Wang, Z. B., De Vries, M. B., & Herman, P. M. J. (2005). Impact of vegetation on flow routing and sedimentation patterns: Three-dimensional modeling for a tidal marsh. *Journal of Geophysical Research*, *110*, F04019. <https://doi.org/10.1029/2005JF000301>
- Townsend, D. W., Pettigrew, N. R., Thomas, M. A., Neary, M. G., McGillicuddy, J., Dennis, J., & O'Donnell, J. (2015). Water masses and nutrient sources to the Gulf of Maine. *Journal of Marine Research*, *73*(3), 93–122. <https://doi.org/10.1357/002224015815848811>
- Valiela, I., Lloret, J., Bowyer, T., Miner, S., Remsen, D., Elmstrom, E., & Thieler, E. R. (2018). Transient coastal landscapes: Rising sea level threatens salt marshes. *Science of the Total Environment*, *640*, 1148–1156.
- Van der Wegen, M. (2013). Numerical modeling of the impact of sea level rise on tidal basin morphodynamics. *Journal of Geophysical Research: Earth Surface*, *118*, 447–460. <https://doi.org/10.1002/jgrf.20034>
- Van der Wegen, M., Dastgheib, A., Jaffe, B. E., & Roelvink, D. (2011). Bed composition generation for morphodynamic modeling: Case study of San Pablo Bay in California, USA. *Ocean Dynamics*, *61*(2–3), 173–186. <https://doi.org/10.1007/s10236-010-0314-2>
- Van Rijn, L. C. (1993). *Principles of sediment transport in rivers, estuaries and coastal seas*, (Vol. 1006, pp. 11–13). Amsterdam: Aqua Publications.
- Vermeer, M., & Rahmstorf, S. (2009). Global sea level linked to global temperature. *Proceedings of the National Academy of Sciences*, *106*(51), 21527–21532. <https://doi.org/10.1073/pnas.0907765106>
- Yang, H. F., Yang, S. L., Meng, Y., Xu, K. H., Luo, X. X., Wu, C. S., & Shi, B. W. (2018). Recent coarsening of sediments on the southern Yangtze subaqueous delta front: A response to river damming. *Continental Shelf Research*, *155*, 45–51. <https://doi.org/10.1016/j.csr.2018.01.012>
- Yang, S. L., Luo, X., Temmerman, S., Kirwan, M., Bouma, T., Xu, K., & Wang, Y. P. (2020). Role of delta-front erosion in sustaining salt marshes under sea-level rise and fluvial sediment decline. *Limnology and Oceanography*. <https://doi.org/10.1002/lno.11432>
- Zhang, S., Luo, Y., Rothstein, L. M., & Gao, K. (2016). A numerical investigation of the interannual-to-interpentadal variability of the along-shelf transport in the Middle Atlantic Bight. *Continental Shelf Research*, *122*, 14–28. <https://doi.org/10.1016/j.csr.2016.03.022>
- Zhang, X., Leonardi, N., Donatelli, C., & Fagherazzi, S. (2019). Fate of cohesive sediments in a marsh-dominated estuary. *Advances in Water Resources*, *125*, 32–40. <https://doi.org/10.1016/j.advwatres.2019.01.003>
- Zhou, X., Zheng, J., Doong, D. J., & Demirebilek, Z. (2013). Sea level rise along the East Asia and Chinese coasts and its role on the morphodynamic response of the Yangtze River Estuary. *Ocean Engineering*, *71*, 40–50. <https://doi.org/10.1016/j.oceaneng.2013.03.014>

UNCORRECTED PROOF